3-D MICRO SWIMMING DRONE WITH MANEUVERABILITY

Fang-Wei Liu and Sung Kwon Cho University of Pittsburgh, Pittsburgh, USA

ABSTRACT

Wirelessly powered and controllable microscale propulsion in 3-D space is of critical importance to micro swimming drones serving as an active and maneuverable in vivo cargo for medical uses. This aritcle describes a 3-D micro swimming drone navigating in 3-D space, propelled by unidirectional microstreaming flow from acoutsically oscillating bubbles. 3-D propulsion is enabled by multiple bubbles with different lengths embedded in different orientations inside the drone body. Each bubble generats propulsion by applying acoustic field at its resonance frequency. Therefore, 3-D propulsion in any direction is achievable by resonating bubbles individually or jointly. The drone with such a complex design was fabricated by a two-photon polymerization 3-D printer. For stable maneuverability, a non-uniform mass distribution of the drone is designed to restore the drone to the designated posture under any disturbances. The restoration mechanism is formulated by a mathematical model, predicting the restoring time and shows an excellent agreemnt with the experimental results. This 3-D micro swimning drone proves its robustness as a manueverable microrobot navigating along programmble path in a 3-D space through selective and joint actuation of microbubbles.

INTRODUCTION

Micro propulsion has been massively studied since it is a critical component of maneuverable microrobots for *in vivo* applications, such as drug delivery, biosensing, and microsurgery [1]. To navigate a microrobot inside human body, the propulsion mechanism should be microscale, controllable in magnitude and direction, and wireless in power supply. The existing methods include external electromagnetic field driving magnetic helical swimmers [2], catalytic reaction by chemical fuel [3], etc.

Among many methods, microstreaming is a competitive candidate which generates a significant and directional flow in microscale. The directional microstreaming using a one-end-sealed glass capillary tube has been first reported for 1-D propulsion [4]. Later, the similar concept has been proved using MEMS (Microelectromechanical Systems) fabricated devices [5, 6]. An air bubble was automatically trapped inside the oneend-open microtube as soon as the hydrophobic microtube was immersed into water. Directional microstreaming was generated by exciting the gaseous bubble trapped in the microtube using an external acoustic wave: the interface of the bubble near the opening of the tube oscillates back and forth at the frequency of the external acoustic field, and thus generates a non-zero time-averaged outgoing microstreaming flow from the opening of the tube. Consequently, the flow exerts a reaction force in the opposite direction as propulsion on the tube. Such microstreaming propulsion provides the advantages of easy actuation, light and simple peripheral devices, wireless transmission, and minimal harm and interference of the actuation signal to living organisms and other medical equipment.

Here, the resonance frequency of the bubble is critically determined by the length of the bubble that is

similar to the length of the tube. This implies selective actuation: only frequency-matched bubbles are activated among a group of multiple bubbles of various lengths. Using this characteristic, 2-D steered propulsion was reported where two groups of microtubes with two different lengths were oriented orthogonally [7, 8]. Each group had its own resonance frequency. One group was used to propel the swimmer while the other was used to steer the direction. By switching the frequency of the acoustic input, a variety of 2-D propelling motion was demonstrated. However, the implementation of the above concept into maneuverable 3-D propulsion has not been reported and brings many challenges. The upmost challenge is 3-D microfabrication with orthogonal alignments of microtubes. Another challenging problem is that maintaining the orientation of the drone suspended in a 3-D space is extremely difficult.

This article presents how we tackle the above challenges to achieve the maneuverable 3-D swimming. Maneuverable 3-D propulsion needs at least three independent propulsions in different directions. For example, one is for the vertical motion to change the elevation while two others is to generate a clockwise/counterclockwise yaw (Fig. 1). Accordingly, three groups of microtubes are incorporated to the 3-D micro drone body. One group is responsible for the upward motion; the downward motion is driven by gravity. The other two groups produce the forward motion when simultaneously actuated as well clockwise/counterclockwise yaw when actuated individually. The complex structure of 3-D micro swimming drone (smaller than 1 mm³ in volume) was fabricated by a two-photon polymerization 3-D printer, which accurately builds hollow microtubes lying on three non-parallel planes inside the drone body.

The second challenge is related to stability in 3-D swimming. As opposed to 2-D swimming where the bottom solid surface serves as a confinement, the bottom surface does not always exist in 3-D swimming. This increased degree of freedom puts the drone in a random orientation after actuations or under disturbances, which makes subsequent actuations difficult. As a result, it is critically important to restore the micro drone in pre-determined posture before each actuation. Hence, a restoring mechanism is incorporated into the drone by carefully redistributing the drone mass: create a mismatch between the center of gravity (CG) and the center of buoyancy (CB). The mismatch always generates a restoring torque to bring

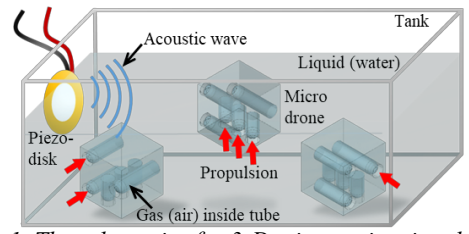


Fig. 1. The schematics for 3-D micro swimming drone with three types of microtubes at different lengths, which enable propulsion in three directions.

the drone to the upright posture. Then, subsequent actuations can be easily determined and programed to achieve desired motions. As a result, such automatic restoration facilitates a stable 3-D swimming performance, which brings the present micro drone closer to practical applications. With these two features, the present micro drone is able to swim in a 3-D space in a stable and maneuverable manner.

EXPERIMENTAL

Fabrication of Micro Swimming Drone

The 3-D microscale drone structure was fabricated by a 3D laser printer utilizing two-photon polymerization (Nanoscribe GmbH, Germany). First, a drop of photoresist (IP-S) was placed on an ITO-coated substrate and cured into designed conformation by the laser. Afterwards, the excessive photoresist was removed by SU8-developer (MicroChem Corp., USA), followed by a rinse of isopropanol (Sigma-Aldrich, USA).

Examination of Restoration of Orientation

The restoring time of the 3-D micro drone was measured in a water-glycerol mixture with the volume ratio of 5:1 (density = 1045 kg/m³, viscosity = 0.0015 N•s/m²). The microtubes in the drone automatically trapped air inside as soon as the drone was immersed in the solution. The microdrone was first suspended in its upright posture (equilibrium state). Then, the micro drone was held by tweezers in a random orientation and then released. The restoration time from the initially disturbed orientation to the upright posture was measured by analyzing the images recorded by a camera (KP-D20AU, Hitachi, Japan).

3-D Swimming with Maneuverability

The micro swimming drone was tested in an acrylic tank $(10 \times 10 \times 5 \text{ cm}^3)$ filled with the same solution above. Two piezoelectric diaphragms (7BB-27-4L0, Murata Electronics, USA) were glued to the sidewalls of the tank and connected to a function generator with an amplifier. The resonance frequency of each type of the microtubes was preliminarily determined by frequency-sweeping experiments under a constant voltage applied. The resonance frequency of each type of tube was determined where the oscillation of the bubble was maximum.

RESULTS

Design of the 3D Micro Swimming Drone

To navigate in 3-D space, three types of microtubes are placed in different orientations and positions inside the drone body (Fig. 2). The length and the number of tubes for each type are as follows: "Lateral 1" (890 μm long × 2), "Lateral 2" (590 µm long × 3), and "Vertical" (470 µm long × 6). A decrease in diameter near the tube opening introduces a physical barrier to fix the interface of the bubble and thus maintains its length during bubble trapping and operation [9]. The individual resonance frequencies of Lateral 1, Lateral 2, and Vertical were 5.9 kHz, 7.9 kHz, and 11.7 kHz. As the propulsion direction is opposite to the outgoing direction of the opening of microtubes, various propulsions can be achieved by solely or jointly actuating the microtubes: (1) propelling upward by Vertical, (2) yawing clockwise or counterclockwise by Lateral 1 or 2 respectively, (3) moving forward by Lateral 1 and 2 simultaneously at 6.3 kHz and (4) downward by gravity. The opening of Vertical tubes is placed above the bottom of the drone to have a room to develop microstreaming flow

for stable taking off/landing on the bottom surface. In addition, a dummy empty tube with both ends open in the top corner is intentionally added to reduce and re-distribute the mass in the upper part of the drone, as discussed in more detail in the next section.

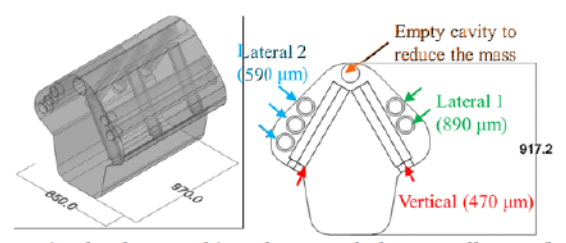


Fig. 2. The design of 3-D drone with the overall view (left) and the front view (right). The diameter of all microtubes is 100 µm (Unit: microns)

Restoration of Orientation

An appropriate mass distribution over the drone body facilitates restoration of drone orientation after actuations or under disturbances. The underlying mechanism is the mismatch between the center of buoyancy (CB) and the center of gravity (CG), as the buoyancy and gravity play influential roles in dynamics at the current scale. The microtubes and the empty tube effectively reduces the local density of the upper part of drone, resulting in the CG locating 22 µm below the CB (Fig. 3). In this configuration, the 3-D micro drone is in equilibrium with its upright posture when the CG is located below CB in gravitational direction (Fig. 3, middle). Whenever any disturbance or propulsion force deviates the drone from this posture, the CG and CB generates a torque to restore the drone to the upright posture by either rolling (Fig. 3, left and right) or pitching (Fig. 4(a)).

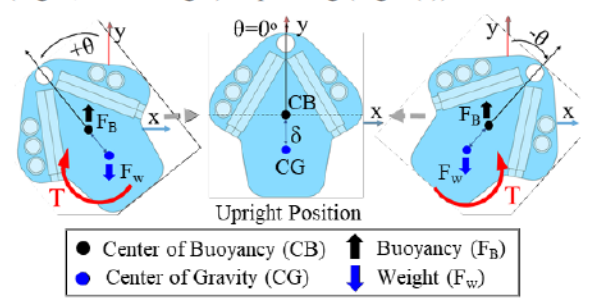


Fig. 3. Orientation restoring mechanism: non-uniform mass distribution restores the drone to the upright posture (middle). The location mismatch between CB and CG generates a restoring torque (T) from disturbed orientations (left and right figures)

The dynamics of restoration can be formulated by the balance of torque about CG:

$$I\frac{d^{2}\theta}{dt^{2}}\rho\ A\mu R^{3}\frac{d\theta}{dt}\rho\ \rho Vg\delta s0n\theta=0 \eqno(1)$$

where *I* is the moment of inertia of rolling $(4.25 \times 10^{-17} \text{ kg} \cdot \text{m}^2)$ or of pitching $(6.58 \times 10^{-17} \text{ kg} \cdot \text{m}^2)$, θ the angular displacement, *A* the rotating drag coefficient obtained experimentally, μ the fluid viscosity $(0.0015 \text{ N} \cdot \text{s/m}^2)$, ρ is the fluid density (1045 kg/m^3) , *R* the equivalent drone size $(456 \mu\text{m})$, *V* the drone volume $(4.9 \times 10^{-10} \text{ m}^3)$, *g* the gravity (9.8 m/s^2) , and δ the distance between CB and CG $(22 \mu\text{m})$.

From Eq. (1), the time constant is derived as:

$$\tau = \frac{2I}{A\mu R^3 - = \overline{\mu A\mu R^3 R^2 - 4I\rho V g \delta}} \tag{2}$$

For the design in Fig. 2, Eq. (2) yields $\tau \approx 0.1$ sec.

The experimental demonstration about restoration of the 3-D micro drone is shown in Fig. 4 (a) and (b) where the drone is initially held by a tweezer in a deviated posture and then restores itself after being released. The averaged (out of 21 trials) time trace of restoration in rolling was measured (normalized angular displacement θ/θ_0 vs. dimensionless time t/τ), as displayed in Fig. 4 (c), and shows an excellent agreement with Eq. (1). All restorations are completed within ~0.4 sec, meaning that a pause longer than 0.4 sec between two actuations assures returning of the drone always to the upright posture before next actuation starts. Based on this, an interval is added in the actuation signal.

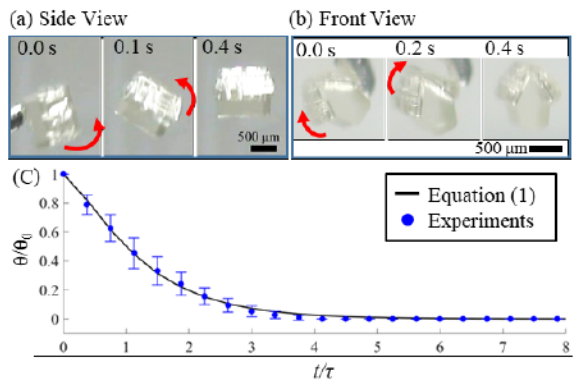


Fig. 4. Restoring results: immediately after tweezers disturb the drone, it completely restores to the upright posture within 0.4 sec: (a) pitch angle restoration and (b) roll angle restoration. (c) restoring behavior in time domain; average data of 21 trials compared with solution to Eq. (1). Time constant $\tau \approx 0.1$ sec.

Maneuverability

The individual propulsions from each type of microtubes are verified by actuating at their own resonance frequencies. The actuation frequency and voltage for the three types of microtubes on the present drone are as followed: (1) Vertical: 11.7 kHz, 58 V, (2) Lateral 1: 5.9 kHz, 22 V, and (3) Lateral 2: 7.9 kHz, 29 V. Figure 5 shows the snapshots. Vertical is able to propel the 3-D micro drone upward by either taking off from the bottom of the tank (Fig. 5(a)) or moving up from any suspended position in a 3-D space. Note that the voltage required for takeoff is usually higher than the one for lifting the drone in a suspended position far away from the bottom surface. Both Lateral 1 and 2 were individually tested on the suspending 3-D micro drone in the solution, where friction effects on the bottom solid surface are absent. The microtubes of Lateral 1 yaws the microdrone counterclockwise (Fig. 5(c)), while the microtubes of Lateral 2 yaws the micro drone clockwise (Fig. 5(b)). This proves that each type of the propulsion can be individually and selectively actuated by applying the resonance frequency of the corresponding microtubes. As mentioned in the previous section, the actuation signal has a duty cycle (switched on 0.43 sec for propulsion and off for 0.57 sec for restoration in each

cycle). The efficacy of the restoration is clearly captured in Fig. 5(a) where the micro drone leans forward while propelling up: pitches at 1.5 sec during the actuations, and then returns to its upright posture during the pause interval at 3.0 sec.

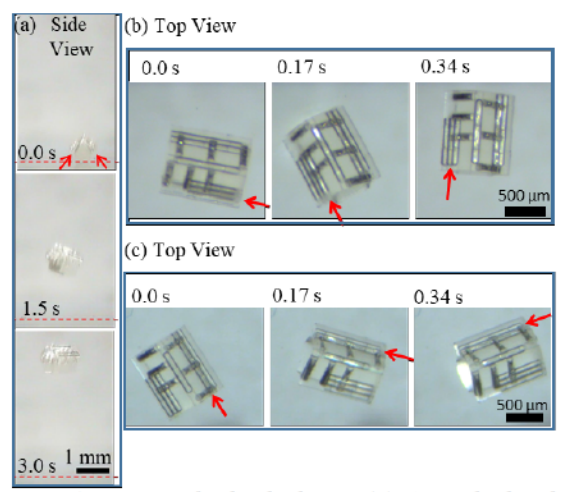


Fig. 5. Activation of individual type: (a) Vertical tubes for propelling upward from the bottom, (b) Lateral 2 for yawing clockwise, and (c) Lateral 1 for yawing counterclockwise. The red arrows indicate activated microtubes.

Consecutive and joint activations of multiple microtubes can generate various paths, navigate the drone in 3-D space, and demonstrate successful maneuverability. Here three different paths are demonstrated. Path 1 consists of 2 actuation steps: activating Vertical followed by the joint actuation of Lateral 1 and 2, as shown in Fig. 6(a). At first, the micro drone is sitting on the bottom at rest. Once Vertical is activated, it takes off from the bottom and elevates to a certain position. Then, the activation is switched to both Lateral 1 and 2 resulting in a forward movement (to the left of the figure). Note that the drone slightly sinks down by gravity during the forward motion. A slight forward displacement during the takeoff is due to the cross-talk, a non-negligible propulsion from nondominant microtubes. Although each type of the microtube has strongest oscillation at its own resonance frequency, it still oscillates at the off-resonance frequencies and generates a minor propelling force as well. This cross-talk is usually observed when the actuation voltage is larger than 48 volts, for example, in the case of takeoff from the bottom surface. However, when the micro drone is suspended in a 3-D space, the propulsive effect is significant even with the actuation voltages below 48 V, and thus the cross-talk rarely appears.

Path 2 shown in Fig. 6(b) is conducted by consecutive actuations of Lateral 2 and then Vertical. First, the microdrone yaws clockwise and simultaneously sinks slowly due to the gravity. Then, the drone stops yawing as soon as Lateral 2 is deactivated. Next, as Vertical is activated, the drone moves upward against the gravity. Path 3 is accomplished by joint activations of all types of microtubes at the same time. The combination of Lateral 1 and 2 results in a forward propulsion along with the upward propulsion by Vertical, as shown in Fig. 6(c). Based on all the results above, the micro swimming drone has the

capability to reach any place in a 3-D space by moving upward, downward, forward, and yawing clockwise and counterclockwise.



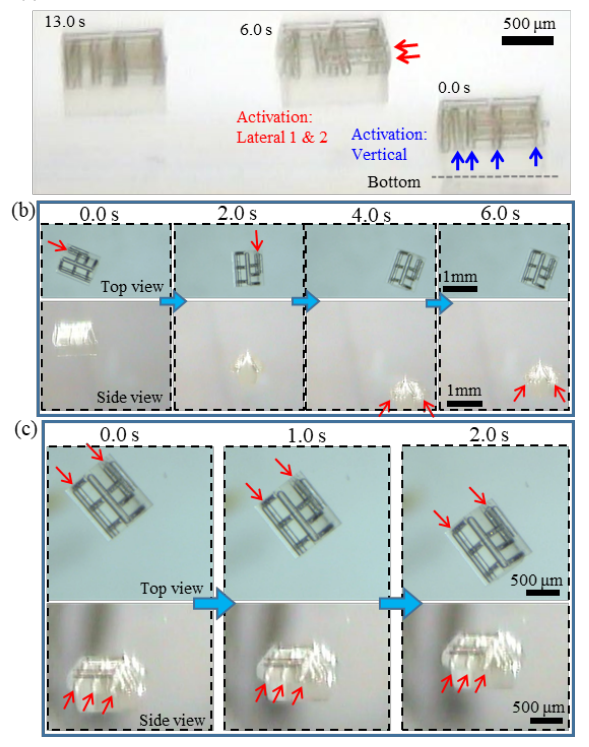


Fig. 6. (a) A superimposed image of consecutive motion: the drone first rests on the bottom surface, then takes off by Vertical tubes (blue arrow) and move left by Lateral 1& 2 tubes (red arrow); Top and side views in (b) and (c) were recorded simultaneously. (b) Consecutive actuation: activation of Lateral 2 resulting in turning counterclockwise but slightly sinking due to gravity. Activating Vertical tubes elevates drone upward (c) Joint actuation: activation of all types of tubes resulting in moving forward straight and upward simultaneously.

CONCLUSION

This article describes a micro swimming drone navigating pre-designed paths in a 3-D space. The drone is propelled by the microstreaming flow generated from the acoustically oscillating cylindrical bubbles. Three groups of microtubes at different lengths are placing on different planes within the drone and responsible for propulsion in upward and forward and clockwise/counterclockwise yaw. The drone moves downward without any propulsion due to the gravity. By switching the acoustic frequency, only selected bubbles are activated when the acoustic frequency matches their resonance frequency. Therefore, the drone can propel in multiple directions in a controlled manner by sole or joint actuation of microbubbles and reaches any position in a 3-D space. An additional unique feature is the restoring mechanism of the drone posture by re-distributing the drone mass to have a mismatch between the center of gravity and the center of buoyancy. This configuration always generates a torques restoring the drone back to the upright posture regardless of external disturbances and previous actuations. This design significantly increases the stability of the drone. Otherwise, the orientation of the drone would be easily disturbed to random positions thus making the following actuations very difficult. A mathematical model was formulated to analyze the restoring dynamics and time showing an excellent agreement with experimental results. This model facilitates to design the actuation signal that has a proper on/off duty cycle. Utilizing these features, a variety of programmed swimming paths are experimentally achieved, demonstrating the maneuverability of the micro swimming drone.

ACKNOWLEDGMENTS

This work was supported by the National Science Foundation (National Robotics Initiatives, ECCS-1637815).

REFERENCES

- J. Feng and S. K. Cho, "Mini and Micro Propulsion for Medical Swimmers," *Micromachines*, vol. 5, pp. 97-113, 2014.
- [2] A. Barbot, D. Decanini, and G. Hwang, "On-chip Microfluidic Multimodal Swimmer toward 3D Navigation," Sci. Rep., vol. 6, p. 19041, 2016.
- [3] S. Sanchez, A. A. Solovev, S. M. Harazim, and O. G. Schmidt, "Microbots Swimming in the Flowing Streams of Microfluidic Channels," *J. Am. Chem. Soc.*, vol. 133, pp. 701-703, 2011.
- [4] R. J. Dijkink, J. P. Van der Dennen, C. D. Ohl, and A. Prosperetti, "The 'acoustic scallop': a bubble-powered actuator," *J. Micromech. Microeng*, vol. 16, pp. 1653-1659, 2006.
- [5] J. Feng and S. K. Cho, "Micro propulsion in liquid by oscillating bubbles," *The 2013 IEEE 26th International Conference on Micro Electro Mechanical Systems (MEMS)*, Taipei, Taiwan, pp.63-66, 2013.
- [6] J. Feng, J. Yuan, and S. K. Cho, "Micropropulsion by an acoustic bubble for navigating microfluidic spaces," *Lab Chip*, vol. 15, pp. 1554-1562, 2015.
- [7] J. Feng, J. Yuan, and S. K. Cho, "2-D steering and propelling of acoustic bubble powered microswimmers," *Lab Chip*, vol. 16, pp. 2317-2325, 2016.
- [8] J. Feng and S. K. Cho, "Two-dimensionally steering microswimmer propelled by oscillating bubbles," *The* 2014 IEEE 27th International Conference on Micro Electro Mechanical Systems (MEMS), San Francisco, CA, USA, pp.188-191, 2014.
- [9] F.-W. Liu, Y. Zhan and S. K. Cho, "Effect of bubble interface position on propulsion and its control for oscillating-bubble powered microswimmer," *The 2018 IEEE 31th International Conference on Micro Electro Mechanical Systems (MEMS)*, Belfast, Northern Ireland, pp. 1173-1176, 2016.

CONTACT

S.K. Cho, tel: +1-412-624-9798; skcho@pitt.edu